Creep and recovery of ultra high modulus polyethylene

M. A. Wilding and I. M. Ward
Department of Physics, University of Leeds, Leeds LS2 9JT, UK
(*Received* 22 *September* 1980; *revised* 23 *December* 1980)

The creep and recovery behaviour of ultra high modulus polyethylene has been studied over the temperature range 20–70°C. Four types of material were examined; low molecular weight and intermediate molecular weight homopolymer, an ethylene hexene-1 copolymer, and a sample prepared by γ-irradiation of isotropic low molecular weight polymer prior to drawing. With the exception of the low molecular weight homopolymer, the materials showed an apparent critical stress below which there was no detectable permanent creep. It is proposed that the behaviour of all the materials can be described to a good approximation by a simple model, where two activated processes are coupled in parallel. Tentative structural explanations of the results are also given.

INTRODUCTION

Previous publications from this laboratory have described the preparation and properties of ultra-high modulus polyethylenes[1-5]. The discussion of properties dealt almost entirely with the 10 second isochronal creep modulus [1,2], or the dynamic mechanical behaviour in extension[5], both measured at very low strains of 0.1% or lower. Under such test conditions, the Young's modulus was shown to be uniquely related to the draw ratio[6]. However, because there was evidence from the initial work that the creep behaviour at high strains depends on the polymer molecular weight as well as the draw ratio[7], and in view of the possible commercial applications of these materials for fibre reinforcement a study was made of the tensile creep and recovery behaviour of LPE. This was described in a recent publication[8], where the investigation centred around a range of monofilament samples of differing draw ratio and molecular weight. Although the viscoelastic behaviour is markedly non-linear it was possible to model the creep and recovery at each individual level of stress by a simple linear solid representation which enabled a clear distinction to be made between recoverable and irrecoverable creep, both of which are affected by draw ratio and molecular weight. The irrecoverable creep was further examined in terms of an activated Eyring process[9], whereupon it was discovered that there is a considerable difference between high and low molecular weight grades. In particular, at high molecular weight there is an apparent critical stress below which irrecoverable creep is negligible. The present paper seeks to extend these findings in order to gain more insight into the physical processes controlling creep. This it does by considering the effects of irradiation-induced cross-linking and of copolymerization. It was found necessary to seek a more comprehensive representation of the creep and recovery behaviour. Following the precedent of the previous publication we have again chosen a very simple model, because it is considered that by avoiding undue complexity it is possible to gain more direct physical insight.

0032-3861/81/070870-07$02.00

EXPERIMENTAL

Preparation of samples

The preparation of spun and drawn monofilaments has been described in detail in a previous publication[8]. For the present study a series of monofilaments was produced by melt spinning at 210°C. The characteristics of these appear in *Table 1*. Also included in this table are some of the samples examined in ref 8. These were used as controls for the irradiated and copolymerized samples. Sample 4 is an ethylene–hexene-1 copolymer having approximately 1.5 butyl side branches per 1000 carbon atoms.

The samples were drawn by stretching between moving rollers which passed the monofilament through a glycerol bath at 120°C. Sample 3 was first subjected to ionizing γ-radiation under glass *in vacuo* at 20°C at a dose rate of 2×10^6 rad h^{-1} to give the final dose shown. A period of four weeks was allowed before this sample was exposed to air, after which it was drawn as above.

Creep measurements

Tensile creep and recovery measurements covering a time range of from 24 to 80 h were performed using the conventional dead-loading apparatus described previously[8] in which the strain was calculated from grip displacement. In the earlier work it was shown that this is an adequate procedure provided that sufficiently long samples are used, so that end effects are negligible. Our previous studies showed that this was true for samples longer than ~5 cm, and therefore a sample gauge length of 10 cm has been adopted. All the measurements were carried out at constant load over a temperature range from 20 to 70°C, the samples being mounted vertically between grips. The temperature was controlled by means of a thermostatic oil bath surrounding the sample. The test filament passed through a central copper tube, which prevented physical contact with the oil. Details of this arrangement are given elsewhere[10]. The extension was determined by means of a linear displacement transducer at the lower grip, and was recorded on punch paper tape

Table 1 Sample details

Sample no.	Polymer grade	$\bar{M}_n$	$\bar{M}_w$	γ-irradiation dose (MR)	Branch content	Draw ratio λ
1(a)	Rigidex 50	6180	101 450	–	–	10
1(b)	Rigidex 50	6180	101 450	–	–	20
2	H020–54P	33 000	312 000	–	–	20
3	Rigidex 50	6180	101 450	2	–	20
4	002–55	16 900	155 000	–	*ca.* 1.5 butyl per 10^3 carbon atoms	20

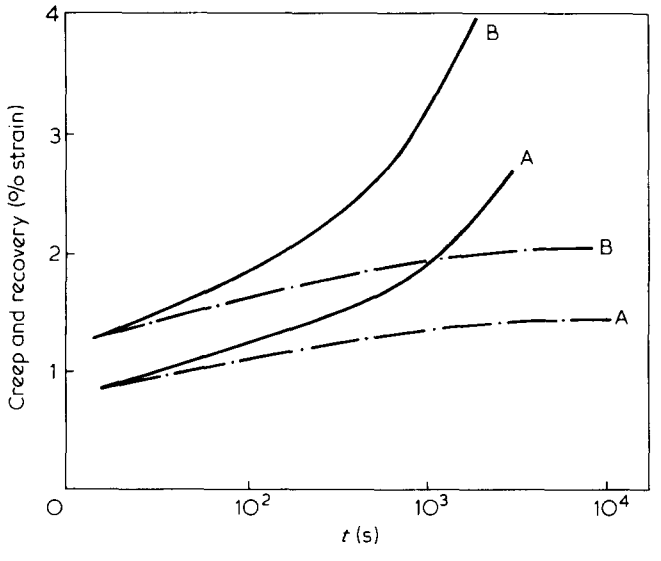

Figure 1 Creep and recovery curves for sample 1(b) at 20°C; —— creep; – – – – recovery; A, 0.15 GPa, B, 0.2 GPa applied stress

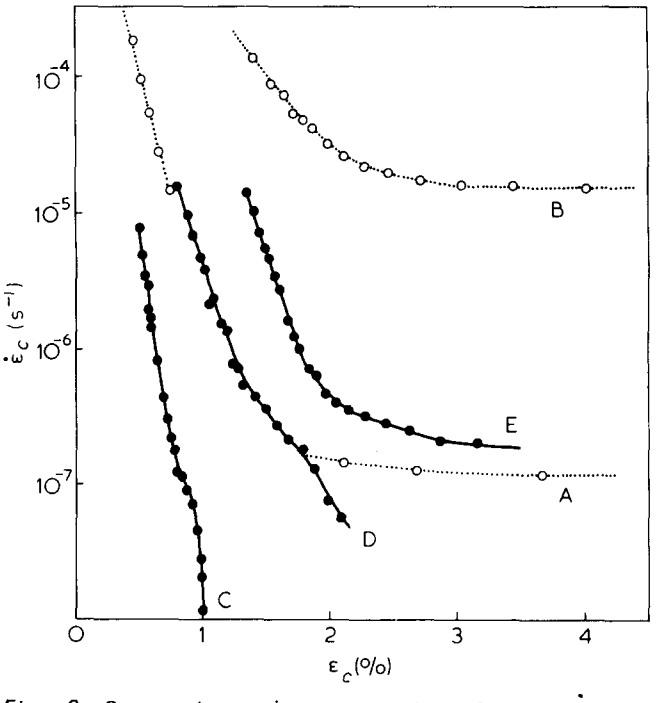

Figure 2 Creep strain rate, $\dot{\epsilon}_C$ vs. creep strain, ϵ_C, for samples 1(b) (– – – –) and 2 (——) at 20°C; A, 0.1 GPa, B, 0.2 GPa, C, 0.1 GPa, D, 0.15 GPa, E, 0.2 GPa

at $\log_2$ (time) intervals. This was facilitated by the use of a binary counting circuit designed in our laboratory. Each sample was tested at several nominal stresses after conditioning in the manner described in ref 8.

RESULTS

Figure 1 shows a set of creep and recovery data for the Rigidex 50 grade material (sample 1(b)) at 20°C. It is clear that a considerable degree of permanent strain is developed, as evidenced by the divergence of the creep and recovery curves at long times. In the previous publication[8] it was shown that this behaviour contrasts sharply with that of a higher molecular weight grade (sample 2) over a similar stress range. This may be illustrated by plotting the creep strain rate ($\dot{\varepsilon}_c$) as a function of the creep strain (ε_c), suggested by Sherby and Dorn[11]. *Figure 2* compares the low and high molecular weight materials. In the case of the Rigidex 50 grade the strain rate ultimately attains a constant level ($\dot{\varepsilon}_p$), which represents the constant flow strain rate after the viscoelastic response has been exhausted. This behaviour has been observed down to the lowest stress levels used. In the previous publication the flow strain rate was associated with the constant rate of extension of a single dashpot of viscosity η_M.

In contrast, the high molecular weight grade does not display a plateau in strain rate except at stresses above ~0.15 GPa. It was also discovered that below this stress the recovery from creep was complete within the resolution of the apparatus. Because of this it was concluded that the low and high molecular weight grades differ in that a 'critical stress' exists in the high molecular weight material, below which the flow process is not activated.

A further, and very significant difference between the two molecular weight grades is that even at high stresses, where permanent flow is seen, $\dot{\varepsilon}_p$ for the high molecular weight material is approximately two orders of magnitude lower than in the low molecular weight grade at the same applied stress (compare for example the 0.2 GPa curves in *Figure 2*).

Figure 3 shows creep and recovery curves for the 002–55 copolymer grade material (sample 4). For the lower stress levels of 0.1 GPa and 0.15 GPa the creep strain rate reduces markedly with increasing time. Moreover the recovery curve is almost coincident with the creep curve, and even at the highest stress level the recovery from strain is almost complete.

Very similar creep and recovery data were obtained for the Rigidex 50 grade material which was irradiated before drawing to draw ratio 20 (sample 3). A useful comparison can be made between the four samples of *Table 1*, the two homopolymers of different molecular weight, the copolymer and the irradiated material. For the same stress level of 0.1 GPa the room temperature creep curves are shown in *Figure 4*, and for a higher stress level of 0.2 GPa Sherby–Dorn plots appear in *Figure 5*.

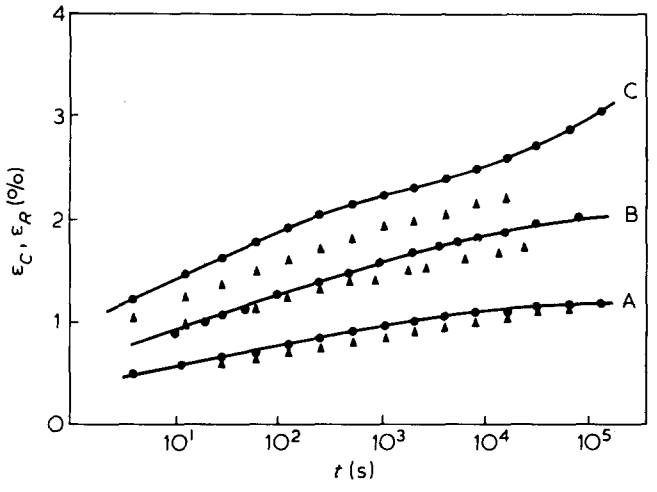

Figure 3 Creep and recovery curves for sample 4 at 20°C; (●) creep; (▲) recovery; A, 0.1 GPa, B, 0.15 GPa, C, 0.2 GPa

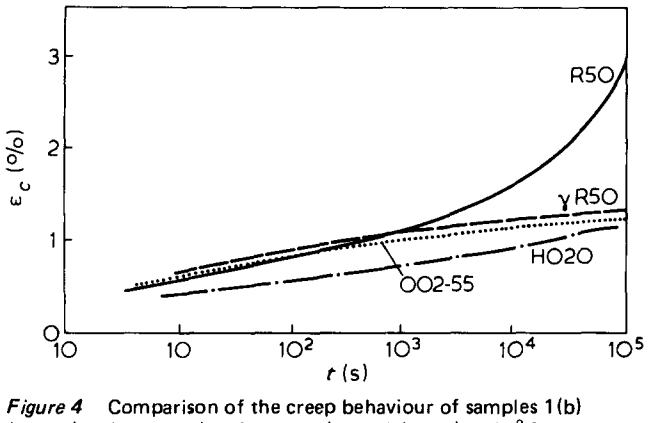

Figure 4 Comparison of the creep behaviour of samples 1(b) (——), 2 (— · — · —), 3 (— — —) and 4 (· · · ·) at 20°C; stress 0.1 GPa

DISCUSSION

General features of creep and recovery behaviour

Figure 4 illustrates the similarity in behaviour of the irradiated polymer, the copolymer and high molecular weight homopolymer. In contrast to the unirradiated Rigidex 50, for all these materials there is an apparent critical stress below which irrecoverable creep does not occur. The simplest representation which would describe the low stress behaviour to a first approximation is the standard linear solid shown in *Figure 6a*. In the previous publication the behaviour of the low molecular weight polymer, where there is irrecoverable flow at all measured stress levels, was shown to be well described by a Maxwell and Voigt element in series (*Figure 6b*). At sufficiently long time the extension of the Voigt element and the Maxwell spring reach their equilibrium value and there is a permanent flow creep described by the Maxwell dashpot. This is the situation which pertains in the plateau regions of the Sherby–Dorn plots. The previous studies showed that the permanent flow could be well represented by an activated rate process as originally proposed by Eyring. Denoting the rate of such a process as before by $\dot{\varepsilon}_p$, then:

$$\dot{\varepsilon}_p = \dot{\varepsilon}_0 \exp(-\Delta_U/kT) \sinh(\sigma V/kT) \qquad (1)$$

where V is the activation volume and ΔU is the activation energy for the process and $\dot{\varepsilon}_0$ is the pre-exponential factor, σ is the applied stress, k is Boltzmann's constant and T is the absolute temperature. The process is therefore characterized by the three parameters V, ΔU and $\dot{\varepsilon}_0$. Although the physical significance of the activation volume is not entirely clear, we consider that it can be associated with the degree of localization of the activated event. At sufficiently high stresses ($\sigma V > 3kT$) the contribution to the back flow term in equation 1 may be ignored, and the activation volume may be obtained by plotting $\log(\dot{\varepsilon}_p)$ as a function of the applied stress at constant temperature.

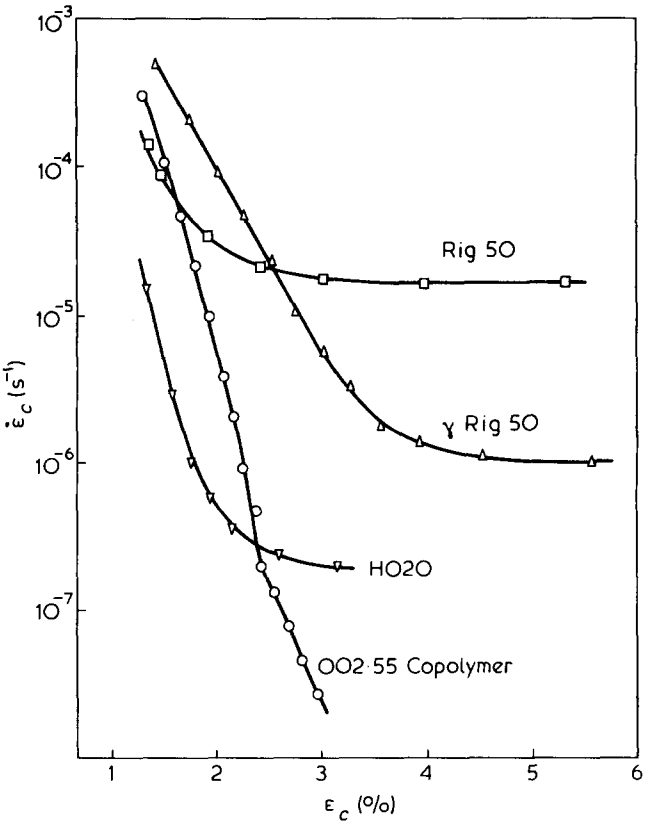

Figure 5 Comparison of $\dot{\varepsilon}_c$ vs. ε_c plots for samples 1(b) (□), 2 (▽), 3 (△) and 4 (○) at 20°C; stress 0.2 GPa

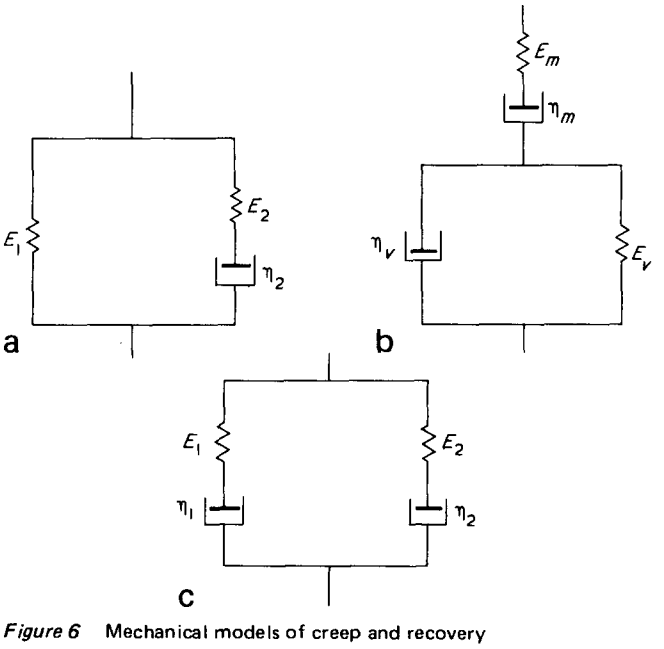

Figure 6 Mechanical models of creep and recovery

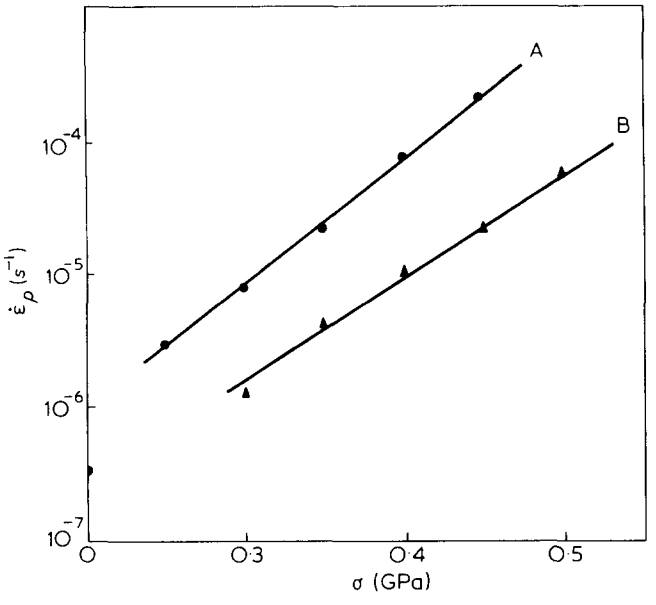

Figure 7 Plateau strain rate, $\dot{\epsilon}_p$, vs. applied stress, σ, at 20°C; A, sample 3; B, sample 4

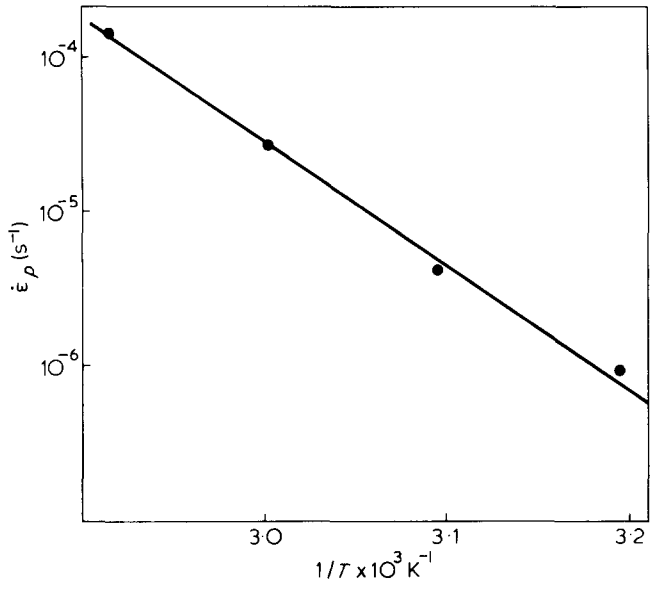

Figure 8 $\dot{\epsilon}_p$ vs. $1/T$ for sample 1(b) at 0.1 GPa applied stress

We have:

$$\log \dot{\varepsilon}_p = \log(\dot{\varepsilon}_0/2) - \frac{\Delta U}{2.3\ \mathrm{k}T} + \frac{\sigma V}{2.3\ \mathrm{k}T} \qquad (2)$$

This plot should be a straight line of slope $V/2.3\,\mathrm{k}T$ for a single Eyring process. As an example, *Figure 7* shows such plots for the irradiated Rigidex 50 grade and the copolymer in the high stress region, in which $\dot{\varepsilon}_p$ was measured from Sherby–Dorn plots. It is seen that in these two polymer grades the creep behaviour above the critical stress is described to a good approximation by a single activated process.

The activation energy, ΔU, may also be obtained from equation 2 since:

$$\log \dot{\varepsilon}_p = \log \dot{\varepsilon}_0/2) - \frac{1}{2.3\ \mathrm{k}T}\{\Delta U - \sigma V\} \qquad (3)$$

For a single activated process, a plot of $\log \dot{\varepsilon}_p$ vs. $1/T$ at constant stress should therefore be a straight line of slope $-\{(\Delta U - \sigma V)/2.3\,\mathrm{k}\}$. Again, as an example, *Figure 8* shows $\log \dot{\varepsilon}_p$ vs $1/T$ for the Rigidex 50 grade material. *Table 2* gives some values of V and ΔU measured for the four polymer grades, assuming a single activated process above the critical stress, and it is clear that there is little distinction between the grades in this respect. They all show very similar activation volumes and activation energies.

The third parameter, the pre-exponential factor, $\dot{\varepsilon}_0$, is generally regarded as relating to the availability of event sites. A convenient method of determining $\dot{\varepsilon}_0$ is to consider the exact form of equation 1. This leads to:

$$\log \dot{\varepsilon}_p = \log \dot{\varepsilon}_0 - \frac{\Delta U}{2.3\ \mathrm{k}T} + \log\{\sinh(\sigma V/\mathrm{k}T)\} \qquad (4)$$

A plot of $\log \dot{\varepsilon}_p$ vs. $\log\{\sinh(\sigma V/\mathrm{k}T)\}$ should be a straight line of unity slope. $\dot{\varepsilon}_0$ may then be calculated from the intercept once ΔU is known. An example of this type of plot for Rigidex 50 at 20°C appears in *Figure 9*, in which the full line is of unity slope.

Finally, because we have found that ΔU does not vary significantly from one grade to the next (see *Table 2*), we have simplified equation 1 as follows:

$$\dot{\varepsilon}_p = \dot{\varepsilon}_0' \sinh(\sigma V/\mathrm{k}T) \qquad (5)$$

where $\dot{\varepsilon}_0' = \dot{\varepsilon}_0 \exp(-\Delta_U/\mathrm{k}T)$

Table 2 Approximate values of 'critical' stress and activation parameters, assuming a single Eyring process above the critical stress

Sample	σ_c at 20°C (GPa)	V at 20°C (Å^3)	ΔU (approx.) (Kcal mol^{-1})	$\dot{\epsilon}_0' = \dot{\epsilon}_0 \exp \Delta U/kT$ (s^{-1})
1(b)	<0.05	87	37	5×10^{-7}
2	0.2	50	31	4.2×10^{-8}
3	0.15–0.2	85	39	3.2×10^{-8}
4	0.25–0.3	70	42	1.8×10^{-8}

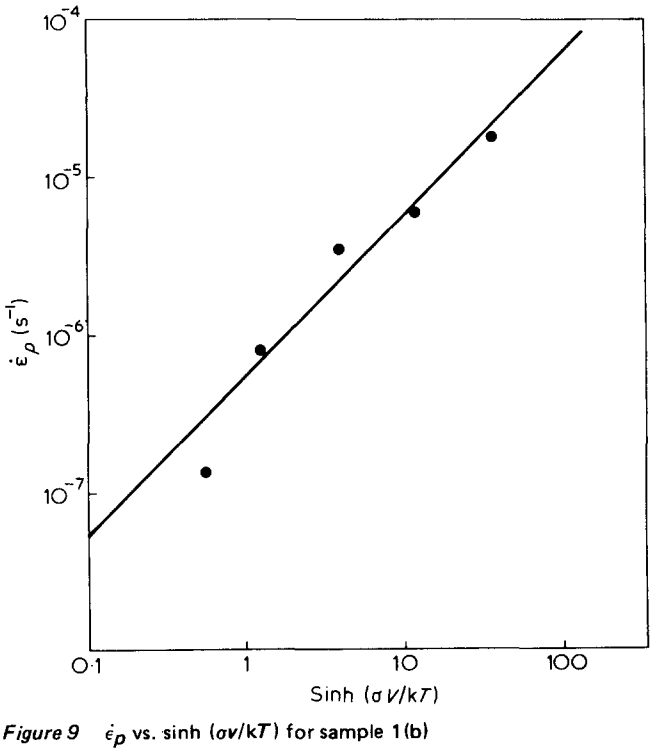

Figure 9 $\dot{\epsilon}_p$ vs. sinh ($\sigma v/kT$) for sample 1(b)

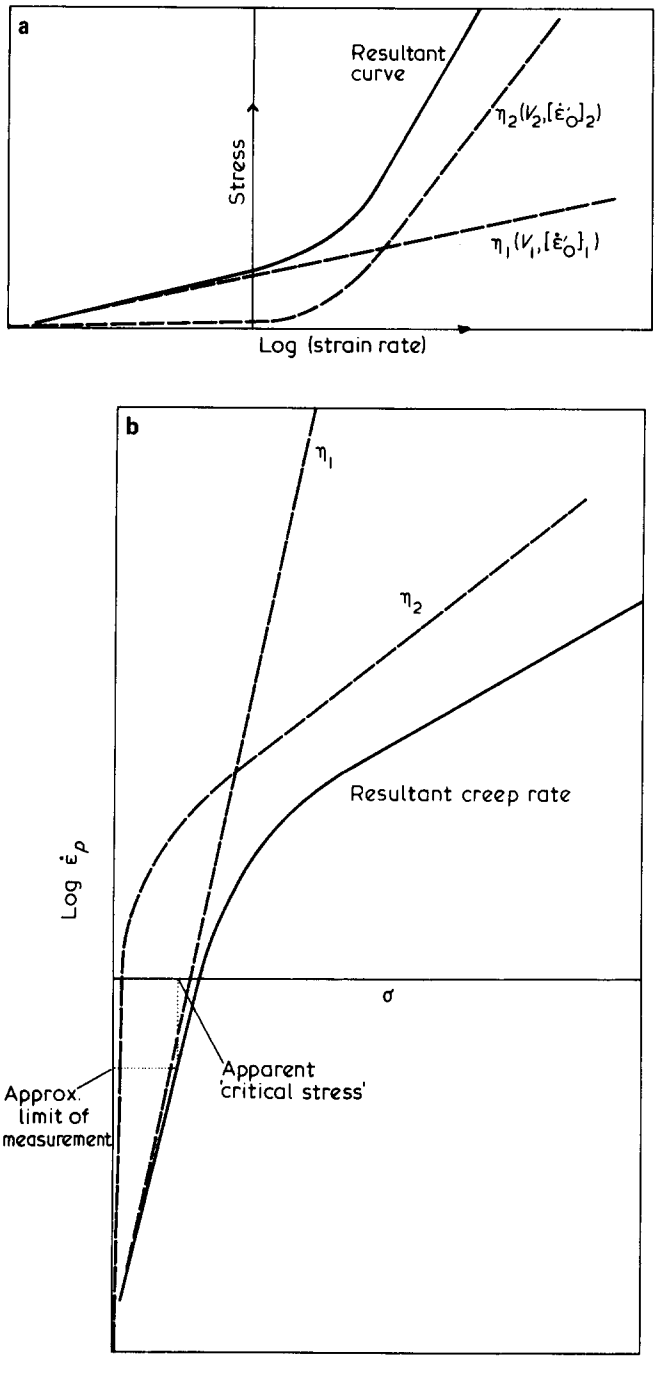

Figure 10 Schematic representation of plastic flow for the 2-process model; (a) yield stress vs. applied strain rate; (b) creep strain rate, $\dot{\varepsilon}_p$ vs. applied stress

Moving on from the situation at high stresses, we now propose that a representation which provides a good description of the permanent flow behaviour of all samples at all stress levels is that shown in *Figure 6c*. The behaviour of both dashpots is considered to follow an activated rate process, as discussed above, and described by equation 1.

The behaviour of the dashpot η_2 is similar to the dashpot η_M in model 6(b), i.e. this dashpot governs the high stress response, and has a comparatively small activation volume. The dashpot η_1, however, has a comparatively large activation volume but a smaller factor $\dot{\varepsilon}'_0$. The behaviour is shown schematically in *Figure 10* where the separate contributions of the two processes are shown together with the total response. In *Figure 10a* we have plotted strain rate on the abscissa and stress on the ordinate which is the more readily recognisable form for the strain rate dependence of a stress activated process, as previously proposed by Roetling[12] and Bauwens[13] for the yield behaviour of glassy polymers. The large activation volume for the dashpot η_1 means that σV_1 is generally large compared to kT and we can use the experimental approximation of equation (2) for this process. The total stress σ is then given by:

$$\sigma = \frac{2.3kT}{V_1}\left(\log \dot{\varepsilon}_p - \log([\dot{\varepsilon}'_0]_1/2)\right) + \frac{kT}{V_2}\sinh^{-1}\left(\dot{\varepsilon}_p/[\dot{\varepsilon}'_0]_2\right) \quad (6)$$

where $[\dot{\varepsilon}'_0]_1$ and $[\dot{\varepsilon}'_0]_2$ are defined in a similar manner to $\dot{\varepsilon}'_0$. In *Figure 10b* we plot strain rate on the ordinate and stress as the abscissa which is the more useful form for considering the present creep data.

At low stress levels, because the viscosity of the dashpot η_1 is much larger than that of the dashpot η_2, we can regard η_1 as infinite and model 6(c) reduces to model 6(a). This is essentially the Eyring formulation of the standard linear solid which was shown to provide a good empirical fit to the creep behaviour of several polymer systems by Eyring, White and Halsey[14].

At high stresses, however, both dashpots are activated by the applied stress. Because of its smaller activation volume the η_2 dashpot takes most of the stress, and hence determines the overall strain rate to a good approximation. After the initial stage of creep both springs are extended to their equilibrium extension and there is permanent flow, the magnitude of which is largely determined by the dashpot η_2. Under these conditions model 6(c) is equivalent to model 6(b) with $\eta_2 = \eta_M$.

At long times the stress in each of the two dashpots is constant, so that all the deformation which arises is permanent plastic strain. Because the stress does not vary, model 6(c) becomes equivalent to a single dashpot of viscosity $(\eta_1 + \eta_2)$. It can easily be shown then that the recovery behaviour is approximately as described by model 6(b). A more detailed analysis requires a complicated integration in the short time region where the stress does vary (and hence, the sinh function is applicable).

Quantitative evaluation of the creep behaviour and its relationship to structure

It is not possible to perform a truly quantitative analysis of the creep behaviour from our existing results, owing to the fact that permanent strain rate measurements cannot be made reliably much below the apparent 'critical stress' i.e. where the long time creep rate apparently falls to zero. However, some indication of the various parameters may be obtained by visually extrapolating the log $(\dot{\varepsilon}_p)$ vs. σ curves to small stresses. Such extrapolations suggested that it was reasonable to assume that the activation volumes for the process represented by η_1 in *Figure 6c* were similar for all samples over the temperature range studies. Furthermore, from the analysis of the high stress data it also appeared that at a given temperature the activation volumes and activation energies for the η_2 dashpot were comparable. We have therefore proceeded on the assumption that the activation

Table 3 Estimates of activation parameters for the 2-process model, assuming a fixed value of V_1 (temperature 20°C)

Sample	V_1 (Å^3)	$[\dot{\epsilon}_0']_1$ (s^{-1})	V_2 (Å^3)	$[\dot{\epsilon}_0']_2$ (s^{-1})2
1(a)	520	*ca.* 10^{-10}	121	*ca.* 10^{-4}
1(b)	520	5×10^{-16}	104	3.5×10^{-5}
2	520	2.6×10^{-22}	55	1×10^{-5}
3	520	*ca.* 10^{-19}	101	*ca.* 10^{-6}
4	520	$<10^{-22}$	80	*ca.* 10^{-7}

volumes for the η_1 dashpot are identical for the four polymers. On this basis, estimates of all the parameters are given (*Table 3*) consistent with the log $\dot{\epsilon}_p$ vs. σ plots. The changes in behaviour due to draw ratio and molecular weight can be attributed mainly to changes in the factors $[\dot{\epsilon}_0']_1$ and $[\dot{\epsilon}_0']_2$.

The activation volume for the η_2 dashpot is in the range 50–100 Å^3 and, as remarked in our previous publication[8], this comparatively small activation volume could be associated with a slip process in the crystalline regions. It is consistent with previous studies of the dynamic mechanical behaviour to identify this process with the α-relaxation process. In previous publications[5] we have discussed the mechanical behaviour of ultra high modulus LPE in terms of a Takayanagi model[15] where the major contributions to the stiffness at temperatures above -50°C comes from the crystal continuity provided by crystalline bridges which link the lamellar stacks in a random fashion. At high temperatures, i.e. in the α relaxation region, the modulus falls because shear of chains past each other in the crystalline regions reduces the effectiveness of the crystalline bridges in transmitting stress. We have drawn an analogy with a short fibre reinforced composite where shear in the matrix reduces the stress transfer between fibres and the matrix. The actual movement of the chains through the crystalline regions must require the presence of defects; the movement of a Reneker defect is one possibility. As the draw ratio increases the molecular chains are straightened out and such defects become less frequent. Thus it would be expected that $[\dot{\epsilon}_0']_2$ would decrease with increasing draw ratio.

The activation volume of ~ 500 Å^3 for the η_1 process is much larger than that for the η_2 process. This is closer to values observed for amorphous polymers, and we would propose that η_1 is associated with the oriented non-crystalline regions. This fits in with our previous interpretation of the mechanical behaviour on a Takayanagi model where we regarded the crystalline bridges as being in parallel with the non-crystalline material and the remaining lamellar material which are in series.

The effects of molecular weight, irradiation and copolymerization can be seen to produce comparatively minor changes in $[\dot{\epsilon}_0']_2$. This agrees with previous work in the sense that the development of the crystalline bridges (and hence the high stiffness) is primarily dependent on draw ratio. In this respect one would expect all the present samples to be comparable. There are minor changes in the direction of reducing $[\dot{\epsilon}_0']_2$ which will relate to reducing the crystal slip process, perhaps because of a molecular entanglement, a crosslink, or a branch point at the surface of the crystal. The major effect is, however, the reduction in $[\dot{\epsilon}_0']_1$ by several orders of magnitude. It is this reduction which reduces the creep at low stresses in a remarkable fashion and gives excellent recovery. We attribute this to major changes in the non-crystalline regions. It is perhaps not too surprising that increasing molecular weight and irradiation cross-linking produce similiar effects. Both can be expected to give rise to network junction points by molecular entanglements and chemical cross-links respectively and both could reduce creep processes. The effectiveness of a small degree of copolymerization is more surprising.

Recovery behaviour

The main features of the recovery behaviour are that after creep at low stresses almost complete recovery is seen, while at high stresses there is a considerable amount of irrecoverable flow. At all stresses model 6(a) predicts complete recovery with a retardation time

$$\tau = \frac{(E_1 + E_2)}{E_1 E_2}\eta_2$$

which reduces to η_2/E_1 for $E_2 \gg E_1$. Model 6(b) is a better representation of the high stress behaviour, but requires the dashpot η_M to be inoperative below some critical stress in order to predict complete recovery.

Model 7(c) displays the correct behaviour for both conditions. At high stresses, steady state flow occurs with the load shared by the dashpots η_1 and η_2 resulting in appreciable permanent strain. At low stresses the dashpot η_1 (high V, low $\dot{\epsilon}_0'$) carries almost the entire load as does E_1. In recovery the conditions are still such that $\eta_1 \gg \eta_2$. Therefore the recovery occurs in the dashpot η_2, driven by E_1, with characteristic time η_2/E_1, which is similar to the behaviour of model 6(a). The dashpot η_1 will contain the permanent strain which may be calculated from the parameters of *Table 3*. It is found that only a small fraction of the total strain is not recoverable. Hence, we would expect to see almost complete recovery, as described by model 6(a). This is certainly borne out by experiment at stresses below the apparent critical stress.

As an example of this we have made the following calculation based on parameters from *Table 3*. From our previous work[8] it can be estimated that the apparent critical stress for H020 at 20°C is ~ 0.2 GPa. Thus, 0.1 GPa is certainly in the region where the η_1 process dominates. Using the parameters of *Table 3* (i.e. extrapolating the data assuming a linear log $\dot{\epsilon}_p/\sigma$ plot at low stress), it can be calculated that for a stress level of 0.1 GPa, $\dot{\epsilon}_p$ is $\sim 10^{-12}$ s^{-1}. Thus, after a creep period of 10^5 seconds (approximately 1 day), the permanent strain developed is approximately 10^{-7} (or 10^{-5}%).

For a typical sample length the smallest strain reading measurable on the creep apparatus is $\sim 5 \times 10^{-3}$%. Thus, the first reliable reading would require 500 days creep. This is well beyond the time scale of any of the tests performed in the present study. Since the total strain developed (including elastic and viscoelastic contributions) at 0.1 GPa is of the order of 1% then the recoverable strain after 500 days creep would be $(1-0.005)\% = 9.95 \times 10^{-1}$%, which represents 99.5% recovery.

We can say that model 6(c) at low stresses is equivalent to model 6(a) (or 6(b) below the 'critical stress'). The apparent critical stress can now be explained satisfactorily. *Figure 10b* shows a schematic representation of the creep response of model 6(c) (flow strain rate vs. stress), in

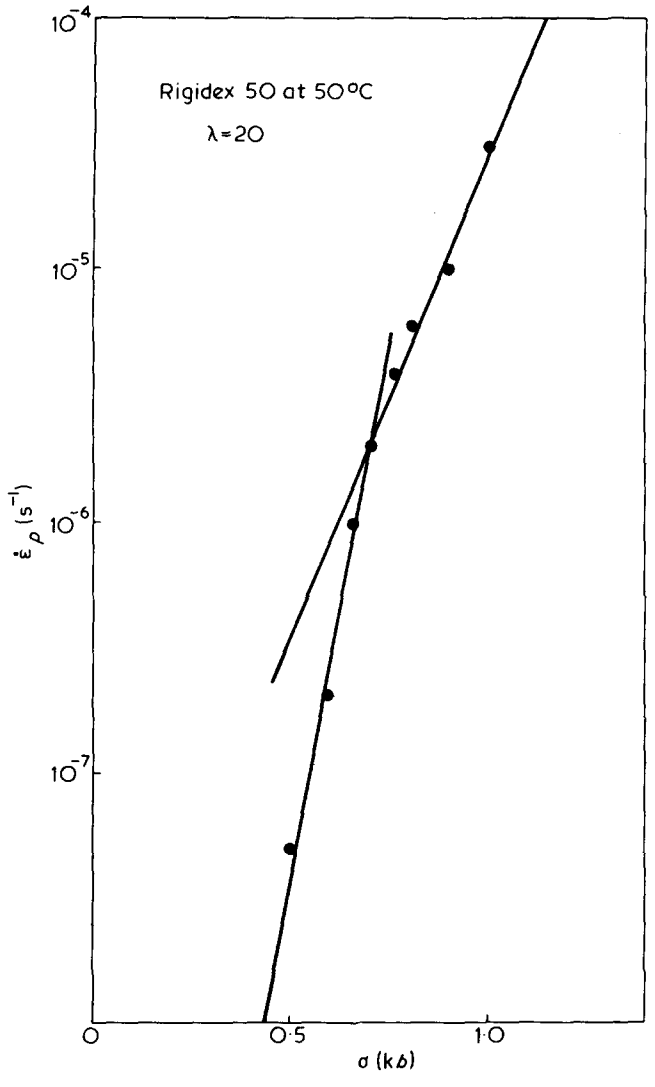

Figure 11 $\dot{\epsilon}_p$ vs. σ for sample 1(b) at 50°C

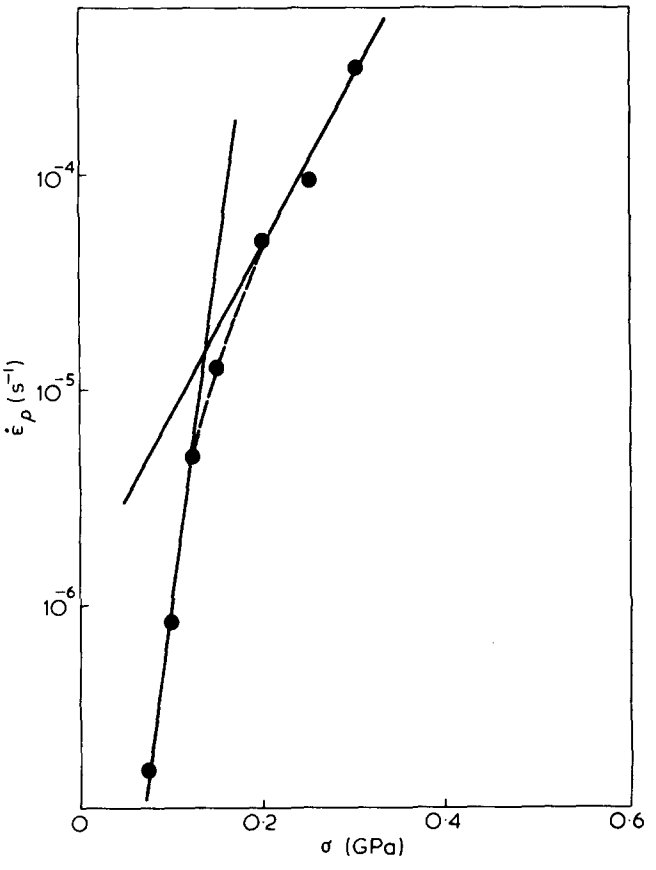

Figure 12 $\dot{\epsilon}_p$ vs. σ for sample 2 at 60°C

which the contributions of the two processes are added together. Because of the limitations imposed by the test itself, it is not practicable to measure strain rates below $\sim 10^{-9}$ s^{-1}. In this region the log $\dot{\varepsilon}_p$, vs. σ plot for process (2) shows curvature due to the contribution of the back flow term. However, at these strain rates process (1) is still in the region for which this term is negligible owing to the much smaller pre-exponential factor and larger activation volume. Thus, a plot of log $\dot{\varepsilon}_p$ vs. σ for process (1) is a straight line except at much less than measurable strain rates. The combination of the two processes gives rise to the full curve in *Figure 10b*. Because of the practical cut-off at low strain rates this plot indicates an apparent critical stress as shown schematically in this Figure.

Our most recent studies have helped to demonstrate further the applicability of model 6(c) to creep behaviour. By extending the measurements to longer times and by choosing the correct temperature, it has been possible to cover the transition region between the two processes in some detail, and the parameters can now be measured with reasonable accuracy. As examples of this work *Figure 11* shows long $\dot{\varepsilon}_p$ vs. σ for sample 1(b) at 50°C, and *Figure 12* gives a similar plot for sample 2 at 60°C. Both sets of results give a reasonable fit to two different linear regions at low and high stresses respectively, consistent with the two-process model.

REFERENCES

1 Capaccio, G. and Ward, I. M. *Nature (Phys. Sci.)* 1973, **243**, 130, 143; *Polymer* 1974, **15**, 233; Br. Pat. Appl. 10746/73 (filed 6.3.73)
2 Capaccio, G., Crompton, T. A. and Ward, I. M. *Polymer* 1976, **17**, 644; *J. Polym. Sci. (Polym. Phys. Edn.)* 1976, **14**, 1641
3 Gibson, A. G., Ward, I. M., Cole, B. N. and Parsons, B. *J. Mater. Sci.* 1974, **9**, 1193
4 Gibson, A. G. and Ward, I. M. Br. Pat. Appl. 30823/73 (filed 28.6.73)
5 Gibson, A. G., Davies, G. R. and Ward, I. M. *Polymer 1978*, **19**, 683
6 Andrews, J. M. and Ward, I. M. *J. Mater. Sci.* 1970, **5**, 411
7 Capaccio, G. and Ward, I. M. *Third International Conference on Deformation, Yield and Fracture of Polymers, Churchill College, Cambridge*, 1976
8 Wilding, M. A. and Ward, I. M. *Polymer* 1978, **19**, 969
9 Eyring, H. *J. Chem. Phys.* 1936, **4**, 283
10 Morgan, C. J. and Ward, I. M. *J. Mech. Phys. Solids* 1971, **19**, 165
11 Sherby, O. D. and Dorn, J. E. *J. Mech. Phys. Solids* 1956, **6**, 145
12 Roetling, J. A. *Polymer* 1965, **6**, 311
13 Bauwens-Crowet, C., Bauwens, J. C. and Homes, G. *J. Polym. Sci.* 1969, **A 2**, 7, 735
14 Halsey, G., White, H. J. and Eyring, H. *Text. Res. J.* 1945, **15**, 295
15 Takayanagi, M., Imada, K. and Kajiyama, T. *J. Polym. Sci. 1966*, **C15**, 263